HHS Public Access

Author manuscript

ASAIO J. Author manuscript; available in PMC 2018 March 01.

Published in final edited form as:

ASAIO J. 2017 ; 63(2): 223–228. doi:10.1097/MAT.0000000000000481.

Pediatric Artificial Lung: A Low-Resistance Pumpless Artificial Lung Alleviates an Acute Lamb Model of Increased Right Ventricle Afterload

Fares Alghanem[*], **Benjamin S. Bryner**[*], **Emilia M. Jahangir**[*], **Uditha P. Fernando**[*], **John M. Trahanas**[*], **Hayley R. Hoffman**[*], **Robert H. Bartlett**[*], **Alvaro Rojas-Peña**[*,†], and **Ronald B. Hirschl**[*,‡]

[*]Extracorporeal Life Support Laboratory, University of Michigan, Ann Arbor, MI, USA

[†]Section of Transplant Surgery, Department of Surgery, University of Michigan, Ann Arbor, MI, USA

[‡]Section of Pediatric Surgery, Department of Surgery, University of Michigan, Ann Arbor, MI, USA

Abstract

Lung disease in children often results in pulmonary hypertension and right heart failure. The availability of a pediatric artificial lung (PAL) would open new approaches to the management of these conditions by bridging to recovery in acute disease or transplantation in chronic disease. This study investigates the efficacy of a novel PAL in alleviating an animal model of pulmonary hypertension and increased right ventricle afterload.

Five juvenile lambs (20-30 Kg) underwent PAL implantation in a pulmonary artery to left atrium configuration. Induction of disease involved temporary, reversible occlusion of the right main pulmonary artery. Hemodynamics, pulmonary vascular input impedance, and right ventricle efficiency were measured under (A) baseline, (B) disease, and (C) disease+PAL conditions.

The disease model altered hemodynamics variables in a manner consistent with pulmonary hypertension. Subsequent PAL attachment improved pulmonary artery pressure (p=0.018), cardiac output (p=0.050), pulmonary vascular input impedance (Z.0 p=0.028, Z.1 p=0.058), and right ventricle efficiency (p=0.001). The PAL averaged resistance of 2.3±0.8 mmHg/L/min and blood flow of 1.3±0.6 L/min.

This novel low-resistance PAL can alleviate pulmonary hypertension in an acute animal model and demonstrates potential for use as a bridge to lung recovery or transplantation in pediatric patients with significant pulmonary hypertension refractory to medical therapies.

Corresponding Author: Alvaro Rojas-Peña, MD, Extracorporeal Life Support Laboratory, Department of Surgery, University of Michigan, 1150 W. Medical Center Drive, B560 MSRBII/SPC 5686, Ann Arbor, MI 48109, alvaror@med.umich.edu, Tel: 734-615-5357 Fax: 734-615-4220.
alfares@umich.edu; bbryner@umich.edu; jahangir.emilia@gmail.com; upfernan@umich.edu; jtrahana@med.umich.edu; hrhoff@med.umich.edu; robbar@med.umich.edu; rhirschl@med.umich.edu

Conflicts of Interest: None

Keywords

Artificial lung; ECMO; lung transplant; pulmonary artery hypertension

INTRODUCTION

Children requiring lung transplantation often decompensate before suitable lungs for transplant become available. Those patients suffering from pulmonary hypertension are especially vulnerable because they may develop both respiratory failure as well as right heart failure.[1] Many of these children will eventually require mechanical ventilation to support respiratory function; however, positive pressure ventilation is associated with severe complications including pneumonia and ventilator-associated events (VAEs).[2] Prolonged mechanical ventilation can lead to deconditioning and often precludes transplantation. Extracorporeal membrane oxygenation (ECMO) has been used as a salvage therapy, but is not a suitable long-term solution due to its complexity, cost, and correlation with poor post-transplant outcomes.[3]

As an alternative, a paracorporeal pediatric artificial lung (PAL) specifically designed to support infants and small children with chronic lung disease may help bridge these patients over a longer duration until donor lungs become available. The PAL would allow patients to wait for ideally matched donor organs and liberate them from mechanical ventilation, reducing VAEs. Additionally, a low-resistance PAL would offload the right ventricle (RV) by providing an alternative low-resistance flow pathway. Perfusion of the PAL solely by the RV would eliminate the need for a pump with its associated hemolysis, thrombosis, and potential mechanical complications.[4,5] Finally, a paracorporeal PAL would allow for ambulation and physical reconditioning while awaiting transplantation, which has been shown to significantly improve post-transplant outcomes in adults.[6,7] Freely ambulating, ventilator- and pump-free patients would be liberated from the intensive care unit (ICU), and could potentially be discharged to low acuity facilities or even home.

To address this clinical need, we sought to create a novel PAL for bridging children to lung transplantation or recovery. Our laboratory has extensive experience with artificial lung technology and has previously tested an adult low-resistance artificial lung in sheep with a surface area of 1.7 m^2.[8] We adapted this technology to a smaller size (surface area 0.5 m^2) with even lower device resistance and priming volume for the pediatric population. The purpose of this early study was to assess the flow characteristics and function of our prototype PAL in an acute lamb model of pediatric lung disease.

MATERIALS AND METHODS

Device Design

The PAL design is characterized by a radial flow pattern of blood facilitated by a centrally located separator. The oxygenator's rigid housing holds a bundle of uncoated polymethylpentene hollow fibers, held in place with polyurethane potting. The hollow fibers and the potting separate the blood and gas phases – the gas flows on the inside while the

blood surrounds the outside of the fibers. The deoxygenated blood enters the oxygenator through a central blood port, and is then diverted by the separator to flow outward through the fiber bundle, where the gas exchange occurs (surface area of all fibers is 0.5 m^2, priming volume is 65 mL). The oxygenated blood leaves the device through the two ports on either side of the device. The inlet and outlet ports are located on the same end of the bundle for easy connection to the patient's vasculature without lengthy conduits. The artificial lung measures approximately 20 cm in length and 5-8 cm in width (Figure 1A – Note: fiber bundle around separator not shown for clarity).

Since the oxygenator is intended for perfusion by the right ventricle without aid from an external pump, it was essential that the PAL have minimal resistance in order to maximize preferential flow through the device. For this reason, the lung was designed to have two outlet ports, relatively large connectors with an inner diameter of 3/8 inches, as well as a large annular space around the fiber bundle to promote flow shunting throughout the device. The added advantage is the ease of priming and de-airing of the device. Computational fluid dynamics (CFD) modeling was carried out on ANSYS CFX software (Ansys Inc., Canonsburg, PA), using previously published methods.[9] Briefly, blood was modeled as an incompressible Navier-Stoked fluid (dynamic viscosity 0.00345 Pa s, density 1060 Kg/m^3), and the fiber bundle was modeled as a porous media, governed by Darcy's Law (permeability 1×10^{-10} m^2, porosity 0.50). The boundary conditions were as follows: blood inlet flow rate = 0.5 L/min, blood outlet pressure = atmospheric pressure and walls = no slip.

In Vitro Gas Exchange and Pressure Drop

In vitro gas transfer was characterized using previous published methods.[10] Briefly, anticoagulated bovine blood was conditioned to venous conditions (hemoglobin 12±1 g/dL, oxygen saturation 65±5 %, pCO_2 45±5 mmHg, base excess 0±5 mmol/L, pH 7.4±0.1, glucose 200±100 mg/dL, temperature 37±2 °C) and pumped through the oxygenator at variable flow rates ranging from 0.25 to 2.0 L/min. Oxygen flow was set at a blood to gas flow ratio of 1:1, 1:4, and 1:8. Blood samples were taken from the inlet and outlet at each flow rate to determine SO_2, pO_2, pCO_2, pH, and hemoglobin concentration and both oxygen and carbon dioxide transfer were calculated. Rated flow was calculated as the maximum blood flow rate (L/min) that can be oxygenated from venous (65±5 %) to arterial (≥95 %) saturations using a FiO_2 = 1. This was obtained by incrementally increasing the oxygenator blood flow until the outlet blood saturation first drops below 95 %.

In Vivo Animal Experiment

All animals received humane care in accordance with the NIH Guide for the Care and Use of Laboratory Animals. Animal protocols were approved by the University of Michigan Institutional Animal Care and Use Committee (IACUC).

Five juvenile lamb weighing 20-30 Kg were induced with propofol (10 mg/Kg), placed in the right lateral decubitus position, and mechanically ventilated using a Penlon Prima 2 ventilator (Penlon Limited, Abingdon, UK) with the following settings: tidal volume 15 mL/Kg, frequency 12 min^{-1}, fraction of inspired oxygen 75 %. General anesthesia was maintained with inhaled isoflurane (1-3.5 %). An arterial line was placed in the left carotid

artery for blood gas sampling and continuous arterial pressure (P_{ART}) monitoring. A venous line was placed in the left jugular vein for medication and fluid administration (200 mL/hour normal saline).

A left thoracotomy was performed, the ligamentum arteriosum was ligated and divided, and the right pulmonary artery (rPA) was identified and isolated with silicone vessel loops. During disease model conditions, the vessel loops were used to occlude the rPA. Animals tolerated rPA occlusion without the need for vasopressor or inotrope support. An 18 mm ultrasonic perivascular flow probe (Transonic, Ithaca, NY) was placed around the main PA to measure PA Flow (Q_{PA}). A micromanometer pressure catheter (Millar, Houston, TX) was inserted into the pulmonary artery to continuously measure pulmonary artery pressure (P_{PA}).

The animals were anticoagulated with a 100-150 units/Kg sodium heparin bolus and maintained on continuous heparin infusion for a target activated clotting time (ACT) of 200-350 seconds. The PAL was then implanted via two Dacron grafts (Terumo Cardiovascular Group, Ann Arbor, MI) each measuring 10 mm in diameter and 8 cm in length. These grafts were anastomosed to the pulmonary artery and left atrium. The device was connected to the grafts via 3/8 inch inner-diameter polyvinyl chloride tubing. Another 3/8 inch ultrasonic flow probe (Transonic, Ithaca, NY) was placed around the tubing to measure the blood flow to the PAL (Figure 2).

Data Acquisition

Three physiologic conditions were evaluated with each animal in the following order: 1) **Baseline:** prior to PAL attachment; 2) **Disease Model:** rPA occlusion prior to PAL implantation; and; 3) **Disease Model + PAL:** rPA occlusion after PAL implantation.

Pulmonary pressure and flow was collected at a sampling frequency of 1000 Hz for 30 seconds at each condition using AcqKnowledge 4.3 software (BioPAC Systems, Goleta, CA). Fourier analysis was performed on P_{PA} and Q_{PA}, breaking down the waveforms into their respective harmonics. Pulmonary vascular input impedance (the opposition to pulsatile flow and an indicator of cardiac load) was calculated by dividing the amplitudes of P_{PA} and Q_{PA} at each harmonic.[11] Resistance is defined by the impedance at the zero harmonic (Z0), and low-frequency impedance is defined by the impedance at the first harmonic (Z1). Characteristic impedance (Zc), or impedance in the absence of wave reflections, can be estimated by the average impedance between 2 and 12 Hz. Right ventricular efficiency, or flow generated per unit of energy consumed, is estimated by CO/Wt, where CO is the cardiac output and Wt is the total right-side heart power (time-averaged integral of the product of P_{PA} and Q_{PA}).[12] Data was expressed as mean ± standard deviation and data analysis was performed using paired-sample t-tests in SPSS Statistics 20 (IBM, Armonk, NY).

RESULTS

Computational Fluid Dynamics (CFD) Modeling

A representative planar view of the computationally obtained velocity and pressure profiles of the oxygenator are shown. The fiber bundle accounted for the largest pressure drop within

the device. As shown in the velocity vector pattern in Figure 1B, the annular spacing allowed the high velocity blood flow from the inlet to be distributed along the height of the device with minimal resistance before entering the fiber bundle, thereby minimizing the overall pressure drop and maximizing uniform blood flow distribution through the fiber bundle. The uniform distribution of flow is beneficial for both improved gas exchange as well as minimized risk of thrombus formation. As shown in the total pressure panel in Figure 1C, the minimal pressure drop is radially-uniform through the fiber bundle. The results demonstrated that the blood flowed preferentially through the annular spacing, reducing the pressure drop across the device.

In Vitro Gas Exchange and Pressure Drop

Average oxygen transfer at 0.5, 1, and 1.5 L/min across all blood to gas ratios was 27.6±0.4, 42.7±1.7, and 54.5±4.0 mL/min respectively. This translates into an average rated flow across all Qb:Qg's of 0.90 L/min (Figure 3A). There is nearly no variation in oxygen transfer between different Qb:Qg ratios. Assuming an average oxygen metabolism of 4 mL/Kg and average flow through the PAL of 1 L/min, this device can fully support the metabolic demands of children up to 2 years of age and partially support (50% metabolism) children up to 6 years of age. In terms of carbon dioxide removal, at maximum sweep flows the PAL was capable of removing 52 mL/min at 0.5 L/min blood flow, 120 mL/min at 1 L /min blood flow, and 132 mL/min at 1.5 L/min blood flow (Figure 3B). Average resistance across the device was 3.4 mmHg/L/min. (Figure 3C).

In Vivo Animal Experiment

All five animals tolerated both the disease model and PAL attachment. The occlusion of the rPA and induction of disease affected all variables in a manner consistent with pulmonary hypertension (Table 1). PAL attachment averaged flows of 1.3±0.6 L/min and resistance of 2.3±0.8 mmHg/L/min. Following PAL attachment, there were improvements in pulmonary artery pressure (29.3±4.4 vs. 25.2±4.9 mmHg, *p=0.018*), cardiac output (3.7±1 vs. 4.2±1 L/min, *p=0.050*), and RV efficiency (12.0±1.7 vs. 14.0±1.8 L/J, *p=0.001*). Additionally, there was a decrease in impedance across the entire pulmonary vascular impedance spectrum, including a statistically significant decrease in resistance (Z0, *p=0.028*) (Figure 4).

In vivo gas exchange of the device was tested using sweep gas of 100 % oxygen at a rate of two times the artificial lung blood flow rate. Inlet partial pressure of oxygen (pO_2) averaged 65.5±10.1 mmHg, while outlet pO_2 averaged 330±140 mmHg. Inlet oxygen saturation averaged 84±0.8 %, while outlet saturations were invariably 100 %. Partial pressure of carbon dioxide (pCO_2) averaged 48.6±2.4 mmHg at the inlet, and 34.3±12 mmHg at the outlet. These measurements were taken with average animal hemoglobin of 8.4±0.9 g/dL and translate into an average oxygen transfer of 21 mL/min.

DISCUSSION

Despite improvements in the outcomes of patients bridged to lung transplantation using ECMO over the last decade, a subset of children with decompensated respiratory failure and pulmonary artery hypertension still lack viable therapies.[13] These children have typically

required extracorporeal veno-arterial support, which is associated with worse post transplantation clinical outcomes, and in some centers is considered a contraindication to listing for lung transplantation.[14] As an alternative, the development of a paracorporeal artificial lung with low resistance would transform the clinical management of these children. Such a device would serve as a bridge to lung recovery in children with pulmonary conditions in which time is needed for lung growth and repair, and serve as a bridge to lung transplantation in children with progressively fatal pulmonary conditions refractory to optimal medical therapy. This study reports our early progress toward developing such a device and focuses primarily on the short-term efficacy and technical performance of a novel PAL at unloading the right ventricle.

The utility of such a device has already been demonstrated by several case reports in which children were transitioned from ECMO to pump-less paracorporeal lung assist devices (Maquet Quadrox-iD or NovaLung oxygenators) as a bridge to lung transplantation.[14-17] The oxygenators were attached in a pulmonary artery to left atrium (PA-to-LA) configuration, in parallel to the native lung, and were used in children with decompensating respiratory function and pulmonary artery hypertension. Although these reports demonstrated the potential of using paracorporeal lung assist devices, the technique is in part limited due to the lack of a suitable artificial lung. These current lung assist devices are ECMO oxygenators with higher resistances and are poorly suited for ambulation or long-term support. Therefore, a PAL designed expressly for pump-less PA-to-LA implantation in children would improve the management and outcomes of patients with pulmonary hypertension and right heart failure.

Admittedly, the artificial lung is not a new technology. Over the last decade, there has been enormous advances in PA-to-LA adult artificial lungs and RA-to-PA and RA-to-Aorta artificial lung-pumps. Our laboratory has tested an adult sized total artificial lung in a one-month ovine model.[8] However, there has been little progress on pediatric pump-less devices. It is important to simultaneously develop a pediatric version of this device given that a larger percent of children compared to adults who are candidates for lung transplantation suffer from idiopathic pulmonary arterial hypertension and other diseases that induce stress on the right ventricle.[18] Additionally, while all lung transplantation is limited by organ scarcity, the pediatric population (particularly those ≤6 years of age) has longer waiting lists and mortality rates in part associated with difficulty of donor-recipient size matching.[19] Similarly, new RA-to-PA and RA-to-Aorta artificial lung-pumps have undergone impressive pre-clinical testing. These ambulatory oxygenators and right ventricular assist devices demonstrated potential to provide cardiopulmonary support and RV unloading for up to one month.[20,21] However, because they require a mechanical pump, they have increased risk for complications such as circuit thrombosis, hemolysis, and platelet consumption. Additionally, the added complexity of a mechanical pump may limit discharge from the ICU.

Therefore, the current PAL was designed to treat pulmonary hypertension by unloading the RV without the need for a mechanical pump. This design focused primarily on creating a low-resistance flow pattern. The compliance of the artificial lung was of low priority because previous studies have shown that compliance has little effect on the cardiac output when compared with decreasing resistance.[22,23] Additionally, resistance and compliance

have an inverse hyperbolic relationship such that decreasing resistance will increase compliance and decrease the pulmonary vascular impedance.[24] This is evident in our data as the PAL was most effective at decreasing pulmonary artery pressure, increasing cardiac output, and decreasing the zeroth harmonic impedance (which is analogue to resistance), but showed significantly smaller reductions in the first harmonic impedance and the characteristic impedance (which are influenced more by compliance). If compliance was introduced into the device, we would have expected a larger decrease in at these harmonics.

Testing the artificial lung under high afterload situations was especially important in our study because acute deterioration and decompensating heart failure is a common observation in patients with end-stage lung disease. Over the last two decades, the most common indication for lung transplantation in children aged 1 to 5 years old was idiopathic pulmonary arterial hypertension.[18] This is in addition to children with secondary pulmonary hypertension caused by other primary lung diseases such as alveolar capillary dysplasia or pulmonary hypoplasia. Our model of right pulmonary artery ligation is sufficiently severe and produced significant increases in all measured indices of cardiac load.[25] We chose pulmonary artery occlusion because it has been shown to place greater strain on the right ventricle than other animal models of lung disease such as microvascular injury models.[26] Although the degree of afterload we achieved is not equal to those observed in children with end-stage lung disease or idiopathic pulmonary hypertension, it does represent the maximum acute non-fatal increase possible.[27] Following PAL attachment, there was a significant decrease in RV afterload, but not a return to baseline values. We recognize that although our device is low resistance, it is still higher resistance than healthy native lungs and is only capable of alleviating, not resolving, the increased afterload. To return pulmonary artery pressures to normal, a device with significantly lower resistance would be needed. Additionally, at such low pressures, there is also a need to focus on decreasing the resistance of the PA and LA anastomosis – which likely contribute significant resistance to the artificial lung blood flow. Concurrently, our laboratory is developing a mock circulatory loop system to study in vitro vascular access configurations.

This study has two main limitations. First, the artificial lung was implanted into lambs with an acute, rather than chronic, model of pulmonary artery hypertension. Therefore, our model lacks the chronic course of progressive deterioration and arteriopathy that are important clinical features of pediatric pulmonary hypertension. Unfortunately, there is no large animal preclinical model that perfectly recapitulates pediatric pulmonary hypertension. Injecting substances into the pulmonary circulation, (sephalex and eramic beads or serial air embolisms), has been developed as a model in sheep - however, these methods often require weeks or months to develop, pushing the animal out of the appropriate size and age range.[28-30] There are also well-established models such as chronic hypoxia, monocrotaline injury, and genetic manipulation – however, the majority of these methods have only been developed in rats and mice.[31] Therefore, we believe that acute right pulmonary artery occlusion represents an appropriate and inexpensive model suitable for early evaluation of our protoype PAL. Children with chronic lung diseases requiring lung transplantation have had years of right ventricle remodeling, and we recognize that their ventricles will tolerate PAL attachment differently than the animals in our acute study. However, these early results are encouraging and indicate that a low-resistance PAL can unload the RV. Second, this

study does not evaluate long-term blood activation and biocompatibility of the artificial lung. A major limitation to the use of artificial lungs has been clotting and the necessity for frequent device exchanges. This concern is magnified when the artificial lung is placed in parallel to the pulmonary circulation because blood bypasses the pulmonary capillary bed, which acts as a blood filter. Therefore, the risk of embolism into the systemic circulation is significantly increased. Both these limitations will be addressed in future chronic experiments.

In conclusion, PA-to-LA artificial lung implantation can alleviate pulmonary hypertension and increase RV efficiency in an acute juvenile lamb disease model, and our prototype PAL demonstrates potential as a bridge to lung recovery or transplantation in pediatric patients.

ACKNOWLEDGMENT

This research was supported by National Institutes of Health Grant 2RO1 HD015434-29. Authors also acknowledge Terumo Cardiovascular Group for their contribution of graft material.

REFERENCES

1. Hanna BD, Conrad C. Lung transplantation for pediatric pulmonary hypertension. Progress in Pediatric cardiology. 2009; 27(1):49–55.
2. Elizur A, Sweet SC, Huddleston CB, et al. Pre-transplant mechanical ventilation increases short-term morbidity and mortality in pediatric patients with cystic fibrosis. The Journal of heart and lung transplantation. 2007; 26(2):127–131. [PubMed: 17258145]
3. Puri V, Epstein D, Raithel SC, et al. Extracorporeal membrane oxygenation in pediatric lung transplantation. The Journal of thoracic and cardiovascular surgery. 2010; 140(2):427–432. [PubMed: 20538306]
4. Fraser CD Jr, Jaquiss RD, Rosenthal DN, et al. Prospective trial of a pediatric ventricular assist device. New England Journal of Medicine. 2012; 367(6):532–541. [PubMed: 22873533]
5. Chen JM, Richmond ME, Charette K, et al. A decade of pediatric mechanical circulatory support before and after cardiac transplantation. The Journal of thoracic and cardiovascular surgery. 2012; 143(2):344–351. [PubMed: 22143101]
6. Olsson K, Simon A, Strueber M, et al. Extracorporeal membrane oxygenation in nonintubated patients as bridge to lung transplantation. American Journal of Transplantation. 2010; 10(9):2173–2178. [PubMed: 20636463]
7. Rehder KJ, Turner DA, Hartwig MG, et al. Active rehabilitation during ECMO as a bridge to lung transplantation. Respiratory care. 2012 respcare. 02155.
8. Sato H, Hall CM, Lafayette NG, et al. Thirty-day in-parallel artificial lung testing in sheep. The Annals of thoracic surgery. 2007; 84(4):1136–1143. discussion 1143. [PubMed: 17888959]
9. Khanafer KM, Cook K, Marafie A. The role of porous media in modeling fluid flow within hollow fiber membranes of the total artificial lung. Journal of porous media. 2012; 15(2)
10. LaFayette NG, Schewe RE, Montoya JP, Cook KE. Performance of a MedArray silicone hollow fiber oxygenator. ASAIO journal. 2009; 55(4):382–387. [PubMed: 19381081]
11. Milnor WR. Pulsatile blood flow. The New England journal of medicine. 1972; 287(1):27. [PubMed: 4555147]
12. Bittner HB, Chen EP, Kendall SW, Biswas SS, Davis RD, Van Trigt P. Right ventricular function in orthotopic total atrioventricular heart transplantation. The Journal of heart and lung transplantation: the official publication of the International Society for Heart Transplantation. 1998; 17(8):826–834.
13. Hoopes CW, Kukreja J, Golden J, Davenport DL, Diaz-Guzman E, Zwischenberger JB. Extracorporeal membrane oxygenation as a bridge to pulmonary transplantation. The Journal of thoracic and cardiovascular surgery. 2013; 145(3):862–868. [PubMed: 23312979]

14. Hoganson DM, Gazit AZ, Boston US, et al. Paracorporeal lung assist devices as a bridge to recovery or lung transplantation in neonates and young children. J Thorac Cardiov Sur. 2014; 147(1):420–427.
15. Boston US, Fehr J, Gazit AZ, Eghtesady P. Paracorporeal lung assist device: An innovative surgical strategy for bridging to lung transplant in an infant with severe pulmonary hypertension caused by alveolar capillary dysplasia. J Thorac Cardiov Sur. 2013; 146(4):E42–E43.
16. Gazit AZ, Sweet SC, Grady RM, Huddleston CB. First experience with a paracorporeal artificial lung in a small child with pulmonary hypertension. The Journal of thoracic and cardiovascular surgery. 2011; 141(6):e48–e50. [PubMed: 21420104]
17. Hoganson DM, Gazit AZ, Sweet SC, Grady RM, Huddleston CB, Eghtesady P. Neonatal paracorporeal lung assist device for respiratory failure. The Annals of thoracic surgery. 2013; 95(2):692–694. [PubMed: 23336880]
18. Benden C, Edwards LB, Kucheryavaya AY, et al. The Registry of the International Society for Heart and Lung Transplantation: sixteenth official pediatric lung and heart-lung transplantation report—2013; focus theme: age. The Journal of Heart and Lung Transplantation. 2013; 32(10): 989–997. [PubMed: 24054807]
19. Valapour M, Paulson K, Smith J, et al. OPTN/SRTR 2011 annual data report: lung. American Journal of Transplantation. 2013; 13(s1):149–177. [PubMed: 23237700]
20. Wang D, Lick SD, Zhou X, Liu X, Benkowski RJ, Zwischenberger JB. Ambulatory oxygenator right ventricular assist device for total right heart and respiratory support. The Annals of thoracic surgery. 2007; 84(5):1699–1703. [PubMed: 17954089]
21. Liu Y, Sanchez PG, Wei X, et al. Effects of Cardiopulmonary Support With a Novel Pediatric Pump-Lung in a 30-Day Ovine Animal Model. Artificial organs. 2015
22. Haft JW, Alnajjar O, Bull JL, Bartlett RH, Hirschl RB. Effect of artificial lung compliance on right ventricular load. ASAIO journal. 2005; 51(6):769–772. [PubMed: 16340366]
23. Akay B, Foucher JA, Camboni D, Koch KL, Kawatra A, Cook KE. Hemodynamic design requirements for in series thoracic artificial lung attachment in a model of pulmonary hypertension. ASAIO journal (American Society for Artificial Internal Organs: 1992). 2012; 58(4):426. [PubMed: 22581034]
24. Tedford RJ. Determinants of right ventricular afterload (2013 Grover Conference series). Pulmonary circulation. 2014; 4(2):211. [PubMed: 25006440]
25. Alghanem F, Davis RP, Bryner BS, et al. The Implantable Pediatric Artificial Lung: Interim Report on the Development of an End-Stage Lung Failure Model. ASAIO journal. 2015
26. Calvin JE Jr. Baer RW, Glantz SA. Pulmonary artery constriction produces a greater right ventricular dynamic afterload than lung microvascular injury in the open chest dog. Circulation research. 1985; 56(1):40–56. [PubMed: 3881198]
27. Goldstein BS, Sweet SC, Mao J, Huddleston CB, Grady RM. Lung transplantation in children with idiopathic pulmonary arterial hypertension: an 18-year experience. The Journal of Heart and Lung Transplantation. 2011; 30(10):1148–1152. [PubMed: 21620736]
28. Kim H, Yung G, Marsh J, et al. Endothelin mediates pulmonary vascular remodelling in a canine model of chronic embolic pulmonary hypertension. European Respiratory Journal. 2000; 15(4): 640–648. [PubMed: 10780753]
29. Pohlmann JR, Akay B, Camboni D, Koch KL, Mervak BM, Cook KE. A low mortality model of chronic pulmonary hypertension in sheep. J Surg Res. 2012; 175(1):44–48. [PubMed: 21529838]
30. Perkett E, Brigham K, Meyrick B. Continuous air embolization into sheep causes sustained pulmonary hypertension and increased pulmonary vasoreactivity. The American journal of pathology. 1988; 132(3):444. [PubMed: 3414777]
31. Stenmark KR, Meyrick B, Galie N, Mooi WJ, McMurtry IF. Animal models of pulmonary arterial hypertension: the hope for etiological discovery and pharmacological cure. American Journal of Physiology-Lung Cellular and Molecular Physiology. 2009; 297(6):L1013–L1032. [PubMed: 19748998]

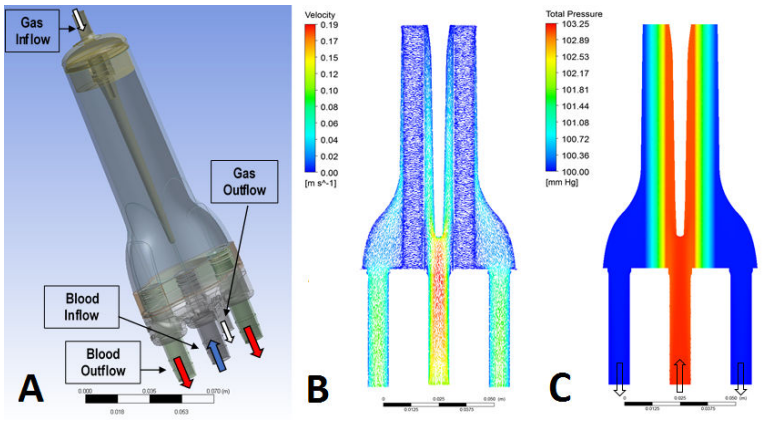

Figure 1. Device design and computational fluid dynamics modeling

A) Schematic of the Device Design; A representative planar view of the computationally obtained velocity (**B**) and pressure (**C**).

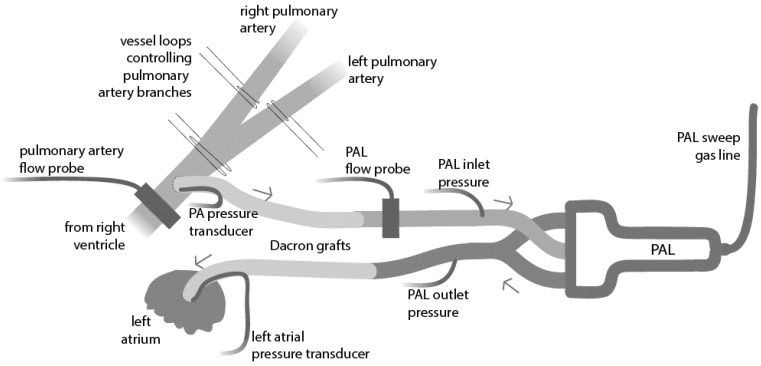

Figure 2.
Experimental setup

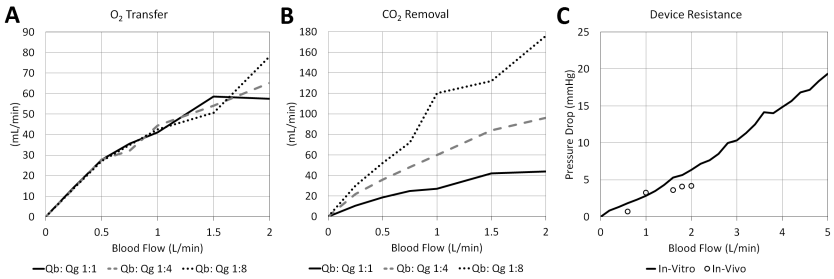

Figure 3. In vitro gas exchange and pressure drop

A) Average oxygen (O_2) transfer; **B)** Average carbon dioxide (CO_2) removal; **C)** Average resistance across the device

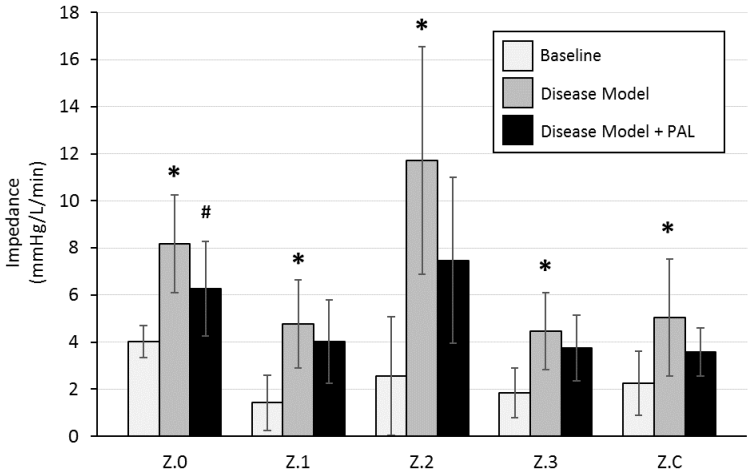

Figure 4. Pulmonary vascular input impedance spectrum

Z.0, zeroth harmonic impedance; Z.1, first harmonic impedance; Z.2, second harmonic impedance; Z.3, third harmonic impedance; Z.C, characteristic impedance. ***** denotes a significant difference between Baseline and Disease Model. **#** denotes a significant difference between Disease Model and Disease

Table 1

In vivo hemodynamics and impedance

				P- Values	
	Baseline	**Disease Model**	**Disease Model + PAL**	***Baseline vs. Disease Model***	***Disease Model vs. Disease Model + PAL***
mP_{ART} *(mmHg)*	66.2 ± 4.2	53.2 ± 9.3	53.2 ± 8.4	*0.009*	*0.496*
mP_{PA} *(mmHg)*	16.7 ± 3.5	29.3 ± 4.4	25.2 ± 4.9	*< 0.001*	*0.018*
mQ_{PA} *(L/min)*	4.3 ± 0.9	3.7 ± 1.0	4.2 ± 1.0	*0.008*	*0.050*
Z.0 *(mmHg/L/min)*	4.0 ± 0.7	8.2 ± 2.1	6.3 ± 2.0	*0.003*	*0.028*
Z.1 *(mmHg/L/min)*	1.4 ± 1.2	4.8 ± 1.9	4.0 ± 1.8	*0.013*	*0.058*
Z.C *(mmHg/L/min)*	2.3 ± 1.4	5.1 ± 2.5	3.6 ± 1.0	*0.025*	*0.146*
CO/Wt *(L/J)*	20.5 ± 2.9	12.0 ± 1.7	14.0 ± 1.8	*0.004*	*0.001*
PAL Flow *(L/min)*	N/A	N/A	1.3 ± 0.6		
PAL Resistance *(mmHg/L/min)*	N/A	N/A	2.3 ± 0.8		

Values are expressed as means ± SD. mP_{ART}, mean arterial pressure; mP_{PA}, mean pulmonary artery pressure; mQ_{PA}, cardiac output; Z.0, zeroth harmonic impedance; Z.1, first harmonic impedance; Z.C, characteristic impedance; CO/Wt, ventricular efficiency; N/A, not applicable.